Structural Engineering and Mechanics, *Vol. 54, No. 5 (2015) 877-890*
DOI: http://dx.doi.org/10.12989/sem.2015.54.5.877

Buckling analysis of functionally graded material grid systems

K. Darılmaz*, M. Gunhan Aksoylu[a] and Yavuz Durgun[b]

Civil Engineering Department, İstanbul Technical University, Maslak, Sarıyer, 34469, İstanbul, Turkey

(Received March 24, 2014, Revised October 9, 2014, Accepted November 15, 2014)

Abstract. This paper aims to fill the technical gap on the elastic buckling behavior of functionally graded material (FGM) grid systems under inplane loads on which few research has been done. Material properties of an FG beam are assumed to vary smoothly in the thickness direction according to power and exponential laws. Based on a hybrid-stress finite element formulation, buckling solutions for FGM grid systems consisting of various aspect ratios and material gradation are provided. The numerical results demonstrate that the aspect ratio and material gradation play an important role in the buckling behavior of FGM grid systems. We believe that the new results obtained from this study, will be very useful to designers and researchers in this field.

Keywords: Grid system; functionally graded materials; buckling; hybrid finite element

1. Introduction

Functionally graded materials (FGMs) are inhomogeneous composites characterized by smooth and continuous variations in both compositional profile and material properties. This continuity prevents the material from having disadvantages of composites such as delamination due to large interlaminar stresses, initiation and propagation of cracks at the interfaces and so on. Thus use of structures like beams, plates and shells, which are made for functionally grade materials (FGMs), have found a wide range of applications in many industries, and to understand the behavior of such systems gained importance.

There have been extensive research carried out in the past years to investigate the behavior and design of FG structures but the literature on the analysis of FG beams is limited when compared with FG plates and shells. Among them the salient works are presented here. Sankar (2001) gave an elasticity solution for transversely loaded functionally graded beam subjected to static transverse loads by assuming that Young's modulus of the beam vary exponentially through the thickness and a simple Euler-Bernoulli beam theory was also developed with the assumption that plane sections remain plane and normal to the beam axis. Chakraborty *et al.* (2003) proposed a new beam finite element based on the first-order shear deformation theory to study the

*Corresponding author, Professor, E-mail: darilmazk@itu.edu.tr
[a]Research Assistant, E-mail: aksoylug@itu.edu.tr
[b]Research Assistant, E-mail: durgunya@itu.edu.tr

http://www.techno-press.org/?journal=sem&subpage=8 ISSN: 1225-4568 (Print), 1598-6217 (Online)

thermoelastic behavior of functionally graded beam structures. In their study, static, free and wave propagation analysis are carried out to examine the behavioral difference of functionally graded material beam with pure metal or pure ceramic. Chakraborty and Gopalakrishnan (2003) analyzed the wave propagation behavior of FG beam under high frequency impulse loading, which can be thermal or mechanical, by using the spectral finite element method. Qian and Ching (2004) used a meshless method to study the free and forced vibration of an FG cantilever beam. Lu and Chen (2005) investigated the Free vibration of orthotropic functionally graded beams, whose material properties can vary arbitrarily along the thickness direction, is investigated based on the two-dimensional theory of elasticity. Zhong and Yu (2007) studied the problem of a cantilever functionally graded beam subjected to different loads and presented a general solution of a cantilever functionally graded beam with arbitrary graded variations of material property distribution based on two-dimesional theory of elasticity. Xiang and Yang (2007) studied the free and forced vibration of an FG beam with variable thickness under thermally induced initial stresses based on the Timoshenko beam theory. Aydogdu and Taskin (2007) developed an equation of motion for functionally graded beam by using Hamilton principle. In these the Young's modulus is assumed to vary along the thickness. Higher order shear deformation theories and classical beam theories were used for the analysis of the FG beam. Ying *et al*. (2008) obtained the exact solutions for bending and free vibration of FG beams resting on a Winkler-Pasternak elastic foundation based on the two-dimensional elasticity theory by assuming that the beam is orthotropic at any point and the material properties vary exponentially along the thickness direction. Kapuria *et al.* (2008) presented a finite element model for static and free vibration responses of layered FG beams using an efficient third order zigzag theory for estimating the effective modulus of elasticity, and its experimental validation for two different FGM systems under various boundary conditions. Yang and Chen (2008) studied the free vibration and elastic buckling of FG beams with open edge cracks by using Euler-Bernoulli beam theory. Li (2008) proposed a new unified approach to investigate the static and the free vibration behavior of Euler-Bernoulli and Timoshenko beams. In a recent study by Yang *et al*. (2008), free and forced vibrations of cracked FG beams subjected to an axial force and a moving load were investigated by using the modal expansion technique. Lü *et al.* (2008) presented elasticity solutions for bending and thermal deformations of bi-directional functionally graded beams with various end conditions using the state space-based differential quadrature method. Şimşek and Kocatürk (2009) investigated the free vibration characteristics and the dynamic behavior of a functionally graded simply supported beam under a concentrated moving harmonic load by using Lagrange's equations under the assumptions of the Euler-Bernoulli beam theory. Şimşek (2010) investigated the vibration analysis of a functionally graded simply-supported beam due to a moving mass by using Euler-Bernoulli, Timoshenko and the third order shear deformation beam theories. Atmane *et al.* (2011) presented a theoretical investigation in free vibration of sigmoid functionally graded beams with variable cross-section by using Bernoulli-Euler beam theory. Cetin and Simsek (2011) analyzed the free vibration of an axially functionally graded (AFG) pile embedded in Winkler-Pasternak elastic foundation within the framework of the Euler-Bernoulli beam theory. Sanjay Anandrao *et al.* (2012) studied the free vibration and thermal post-buckling of shear flexible FGM beams using finite element formulation based on first order Timoshenko beam theory by considering classical boundary conditions. Tajalli *et al*. (2013) developed a formulation for Timoshenko beams made of functionally graded materilas based on the strain gradient theory, and investigated the static bending and free vibration of a FG simply supported beam. Simsek and Reddy (2013) proposed a unified higher order beam theory which is based on the modified couple

stress theory, and investigate the influences the material length scale parameter, aspect ratio, different estimation method of material properties, various material compositions, and the parameters of the elastic medium on the critical buckling load. Li and Batra (2013) derived analytical relations between the critical buckling load of a FGM Timoshenko beam and that of the corresponding homogeneous Euler-Bernoulli beam subjected to axial compressive load for different edge conditions. Bourema *et al*. (2013) developed a new first-order shear deformation beam theory based on neutral surface position for bending and free vibration analysis of functionally graded beams. Kocaturk and Akbas (2013) studied the thermal post-buckling analysis of functionally graded beams with temperature dependent physical properties by using the total Lagrangian Timoshenko beam element approximation. Akgöz and Civalek (2014) presented a shear deformation beam model and new shear correction factors for functionally graded microbeams and solved bending and buckling problems by using Navier solution procedure. Giunta *et al*. (2014) presents a dynamic analysis of three-dimensional functionally graded by hierarchical models. They derived several higher order as well as classicial theories by means of a compact notation for the a-priori expansion order of the displacement field over the beam cross-section. Darilmaz (2015) studied the vibration analysis of FGM grid systems having various aspect ratios, different types of gradations functions and support conditions.

The aim of this paper is to study the influence of aspect ratio, number of divisions, type of gradations functions, type of in-plane loading on the stability of FGM grid systems. Both power law and exponential law are taken for the variation of the material properties through the depth of the beam. A hybrid-stress beam finite element is developed and used in this study.

2. Modeling of FGM properties

Different types of gradations laws are available in the literature. In this study power law and exponential law gradation have been considered in order to calculate the material properties of FG structures. FGM consisting of two constituent materials has been considered. The top surface is assumed to be steel and bottom surface is assumed to be Al_2O_3. The region between the two surface consists of a combination of the two materials with continuously varying mixing ratios of two materials.

The power law for having all the desired properties are introduced by Wakashima *et al*. (1990), is given by

$$P(z) = (P_t - P_b)\left(\frac{z}{h} + \frac{1}{2}\right)^k + P_b \tag{1}$$

$P(z)$ denotes a typical material property (E,G,ρ). P_t and P_b are the corresponding material properties of the top-most and bottom-most surfaces of the beam, and k is the non-negative power-law exponent which defines the material profile through the thickness of the beam.

The exponential law is given by Kim and Paulino (2002) as follows

$$P(z) = P_t e^{-\delta(1-2z/h)} \ , \ \delta = \frac{1}{2}\ln(P_t / P_b) \tag{2}$$

It is evident from Eqs. (1) nd (2) that when $z=-h/2$, $P=P_b$ and when $z=h/2$, $P=P_t$.

The FGM grid system taken into consideration is depicted in Fig. 1.

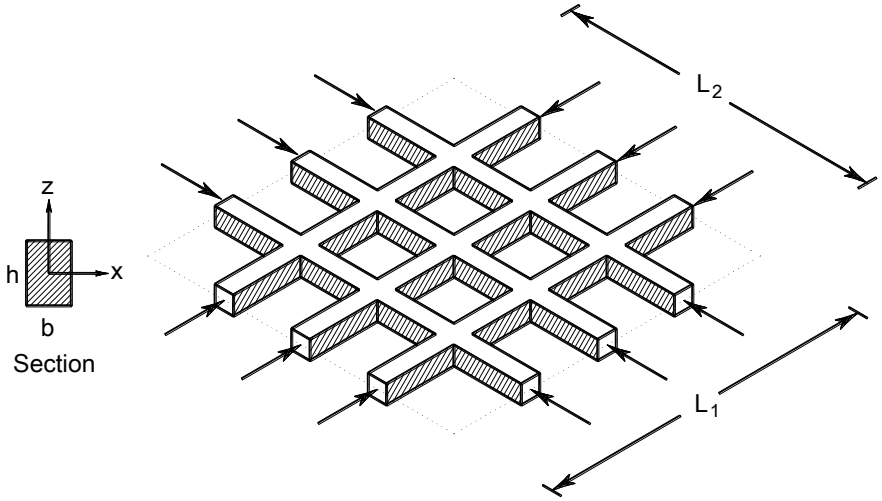

Fig. 1 A functionally graded grid system subjected to in plane loading

3. Finite element formulations

Hybrid-stress finite elements have been developed for the improved analysis based on a modified complementary energy principle in which the intraelement equilibrating stresses and displacements compatible over the entire volume of an element or at the element boundary only are interpolated independently. The element stiffness matrix is obtained using Hellinger-Reissner variational principle in which stresses and displacements are assumed independently (Pian and Chen 1983, Darilmaz 2012) is utilized. This establishes the master fields. Two slave strain fields appear, one coming from displacements and one from stresses.

For a typical beam element whose longitudinal axis is *x*, and *y* and *z* are principal centroidal axes, the Hellinger-Reissner functional can be written as

$$\Pi_{RH} = \int_V \{\sigma\}^T [D]\{u\}\, dV - \frac{1}{2}\int_V \{\sigma\}^T [S]\{\sigma\}\, dV \tag{3}$$

where $\{\sigma\}$ is the vector of assumed stresses, $[S]$ is the material compliance matrix relating strains, $\{\varepsilon\}$, to stress ($\{\varepsilon\}=[S]\{\sigma\}$), $[D]$ is the differential operator matrix corresponding to the linear strain-displacement relations ($\{\varepsilon\}=[D]\{u\}$) and V is the volume of structure. In Eq. (3), the load potential is omitted as it is not required for formulating the element stiffness matrix.

The assumed stress field is described in the interior of the element as

$$\{\sigma\} = [P]\{\beta\} \tag{4}$$

and a compatible displacement field is described by

$$\{u\} = [N]\{q\} \tag{5}$$

where $[P]$ is a matrix which contains the polynomial terms of stress interpolation functions, $[N]$ is a matrix of shape functions, and $\{\beta\}$ and $\{q\}$ are the unknown stress and nodal displacement

parameters, respectively.

Intra-element assumed stresses and compatible displacements are independently interpolated. Since stresses are independent from element to element, the stress parameters are eliminated at the element level and a conventional stiffness matrix results. This leaves only the nodal displacement parameters to be assembled into the global system of equations.

Substituting the stress and displacement approximations Eq. (4), Eq. (5) in the functional Eq. (3)

$$\Pi_{RH} = [\beta]^T [G][q] - \frac{1}{2}[\beta]^T [H][\beta] \tag{6}$$

where

$$[H] = \int_V [P]^T [S][P]\, dV \tag{7}$$

$$[G] = \int [P]^T ([D][N]) dV \tag{8}$$

Now imposing stationary conditions on the functional with respect to the stress parameters $\{\beta\}$ gives

$$[\beta] = [H]^{-1}[G]\ [q] \tag{9}$$

Substitution of $\{\beta\}$ in Eq. (6), the functional reduces to

$$\Pi_{RH} = \frac{1}{2}[q]^T [G]^T [H]^{-1}[G][q] = \frac{1}{2}[q]^T [K][q] \tag{10}$$

where

$$[K] = [G]^T [H]^{-1}[G] \tag{11}$$

is recognized as a stiffness matrix.

The stress stiffness matrix is derived by using the Green-Lagrange strains which correspond to defining the strain of a line segment by the equation

$$\varepsilon = \frac{1}{2}\left[\left(\frac{ds^*}{ds}\right)^2 - 1\right] \tag{12}$$

where ds and ds^* are respectively the initial and final lengths of the line segment.

The nonlinear terms are retained only for the axial strain. The axial strain is written as

$$\{\varepsilon\} = \{\varepsilon_L\} + \{\varepsilon_{NL}\} \tag{13}$$

where the linear part is given by

$$\varepsilon_L = \varepsilon_x = u_{,x} \tag{14}$$

and the nonlinear part is given by

$$\varepsilon_{NL} = \varepsilon_{xNL} = \frac{1}{2}\left(u_{,x}^2 + v_{,x}^2 + w_{,x}^2\right) \tag{15}$$

The bending strains are computed using the changes in curvature by

$$\{\chi\} = \begin{Bmatrix} \chi_x \\ \chi_y \\ \chi_z \end{Bmatrix} = \begin{Bmatrix} \theta_{x,x} \\ \theta_{y,x} \\ \theta_{z,x} \end{Bmatrix} \tag{16}$$

The transverse shear strains are given by

$$\{\gamma\} = \begin{Bmatrix} \gamma_{xy} \\ \gamma_{xz} \end{Bmatrix} = \begin{Bmatrix} v_{,x} - \theta_z \\ w_{,x} - \theta_y \end{Bmatrix} \tag{17}$$

The generalized Hellinger-Reissner functional including the nonlinear strains can be written as

$$\Pi_{RH} = \int_V \{\sigma\}^T [D]\{u\}\, dV - \frac{1}{2}\int_V \{\sigma\}^T [S]\{\sigma\}\, dV + \int_V \{\sigma_o\}^T \{\varepsilon_{NL}\}\, dV \tag{18}$$

where $\{\sigma_o\}$is the prescribed prebuckling stress state. Substituting the stress and displacement approximations in the functional

$$\Pi_{RH} = [\beta]^T [G][q] - \frac{1}{2}[\beta]^T [H][\beta] + \frac{1}{2}\{q\}^T [K_\sigma]\{q\} \tag{19}$$

and stress stiffness matrix is given by

$$[K_\sigma] = \int_V [N]^T (\partial/\partial x)\{\psi\}(\partial/\partial x)[N]\, dV \tag{20}$$

respectively.

The matrix $\{\psi\}$, which corresponds to the pre-buckling stress state, consists of axial stress resultant which is evaluated from a linear static stress analysis. For a grid system $\{\psi\}$ reduced to axial force N.

The field variables (σ and u) take independent variations for the stationarity of $\prod_{RH}$. The strain vector ε is derived from u using strain-displacement relations. Independently assumed generalized stress-resultant vector can conveniently be written in terms of axial, shear, torsion and bending actions as

$$\{\sigma\}^T = \{N, Q_y, Q_z, M_x, M_y, M_z\} \tag{21}$$

Utilizing the strain-displacement relations the generalized strain components in the present beam model can be written as

$$\{\varepsilon\}^T = \{u_{,x}, (v_{,x} - \theta_z), (w_{,x} - \theta_y), \theta_{x,x}, \theta_{y,x}, \theta_{z,x}\} \tag{22}$$

The matrices of interpolation functions for element displacements, stress resultants are polynomial function of the coordinate x. For displacement interpolation functions the compatible displacement functions are used. That is with natural coordinate $\xi = 2x/L$, the interpolation functions for two-noded beam element

$$N_1 = (1-\xi)/2 \quad N_2 = (1+\xi)/2 \tag{23}$$

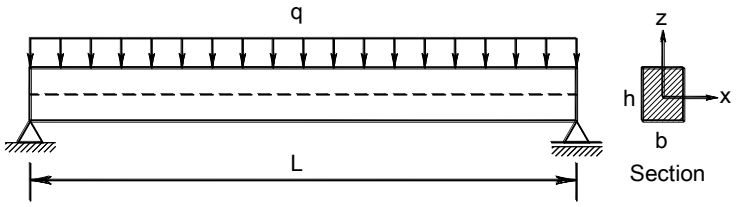

Fig. 2 FG simply-supported beam subjected to uniformly distributed load

For internal force field, the stress parameters are chosen in such a way that the stress equilibrium conditions are satisfied within the element. And also it is recognized that the number of stress modes *m* in the assumed stress field should satisfy

$$m \geq n - r - p \tag{24}$$

with *n* the total number of nodal displacements, *r* the number of rigid body modes and *p* the number of zero-energy modes in an element. If Eq. (24) is not satisfied, use of too few coefficients in $\{\beta\}$, the rank of the element stiffness matrix will be less than the total degrees of deformation freedom and the numerical solution of the finite element model will not be stable and produces an element with one or more mechanisms.

Increasing the number of β's by adding stress modes of higher-order term, each extra term will add more stiffness and stiffens the element, Pian and Chen (1983), Darilmaz (2011). Resulting in the least number of parameters the [*P*] matrix is obtained as

$$[P] = \begin{bmatrix} 1 & 0 & 0 & 0 & 0 & 0 \\ 0 & 1 & 0 & 0 & 0 & 0 \\ 0 & 0 & 1 & 0 & 0 & 0 \\ 0 & 0 & 0 & 1 & 0 & 0 \\ 0 & 0 & x & 0 & 1 & 0 \\ 0 & x & 0 & 0 & 0 & 1 \end{bmatrix} \tag{25}$$

4. Numerical examples

In order to verify the accuracy of presented element a standard static analysis of a FG simply supported beam is carried out. The results obtained are compared with solutions given in Şimşek (2009).

Functionally graded material of the beam is composed of Aluminum (Al; E_{Al}=70 GPa, ν_{Al}=0.3) and Zirconia (ZrO_2; E_{ZrO2}=200 GPa, ν_{ZrO2}=0.3) and its properties changes through the thickness of the beam according to the power-law. The bottom surface of the FG beam is pure Zirconia, whereas the top surface of the beam is pure Aluminum. The width and the thickness of the beam are *b*=0.1 m and *h*=0.1 m, respectively. The length of the beam is taken as *L*=1.6 m. The axial and the transverse displacements of the beam are normalized by the static deflection, $w_{static}=5qL^4/384E_{Al}I$, of the fully aluminum beam under the uniformly distributed load.

Table 1 Maximum non-dimensional transverse deflection of beam

Power-law exponent	Şimşek (2009)	This study
k=0 (*Full metal*)	1.00975	1.00883
k=0.2	0.75737	0.75689
k=0.5	0.64065	0.64011
k=1	0.56699	0.56632
k=2	0.50780	0.50749
k=5	0.44442	0.44424
Full Ceramic	0.35341	0.35306

Table 2 Properties of metallic (Steel) and ceramic (Al_2O_3) phases

Material	Young's modulus E (GPa)	Poisons' ratio	Density kg/m^3
Al_2O_3	390	0.25	3890
Steel	210	0.3	7850

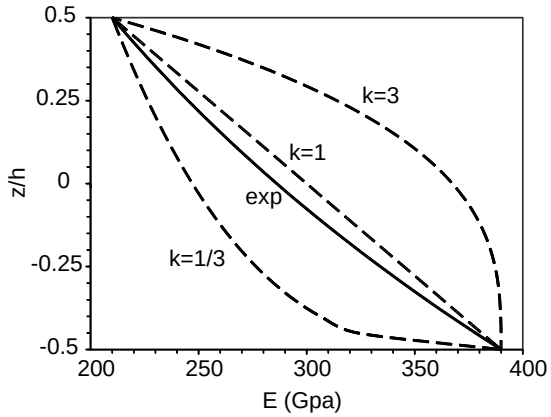

Fig. 3 Variation of the Young's modulus through the thickness of the FG beam

Results showed that the behavior of the present element is satisfactory and results are in a good agreement with solutions given in Şimşek (2009).

In this section six different grid systems are considered by using the above formulation to study the influence of aspect ratio (L_1/L_2), type of gradations functions, distribution of inplane loading on the buckling load of grid system having FGM depicted in Fig. 1. The values of the nondimensional critical load parameter $\lambda=12P_{cr}L_1L_2/(\pi^2E_tbh^3)$ are obtained. The material properties are given in Table 2.

It is assumed that the material properties of the beam vary continously in the thickness direction according to the power-law and exponential form. Fig. 3 shows the variation of Young's modulus in the thickness direction of grid system.

Six different (M1 to M6) grid systems are taken into consideration, Fig. 4. In each case width of the beams is adjusted for keeping the amount of total material constant. For example the width of beam at M4 system is ¼ of the width of beam at M1 system. For M1 system the h/b and b/L_1 ratios are 0.5 and 0.1, respectively. Each line segment is modeled by using 20 finite elements. The

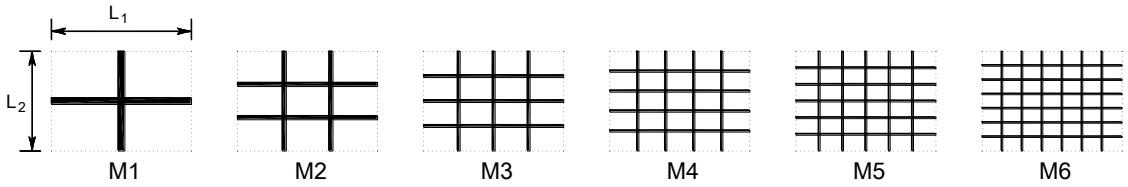

Fig. 4 FG Grid systems

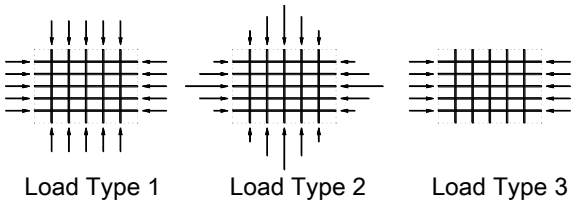

Fig. 5 Loading types

Table 3 Nondimensional buckling load parameter λ, (L_1/L_2=1.0), Load type 1

	k=1/3	k=1	k=3	exp	Steel	Al_2O_3	Steel ANSYS
M1	5.861	6.559	7.232	6.429	4.732	8.788	4.711
M2	6.406	7.360	8.366	7.167	5.089	9.452	5.063
M3	6.345	7.318	8.368	7.120	5.030	9.342	4.997
M4	6.233	7.160	8.148	6.974	4.954	9.200	4.927
M5	6.147	7.027	7.949	6.853	4.899	9.098	4.846
M6	6.085	6.929	7.799	6.764	4.861	9.027	4.823

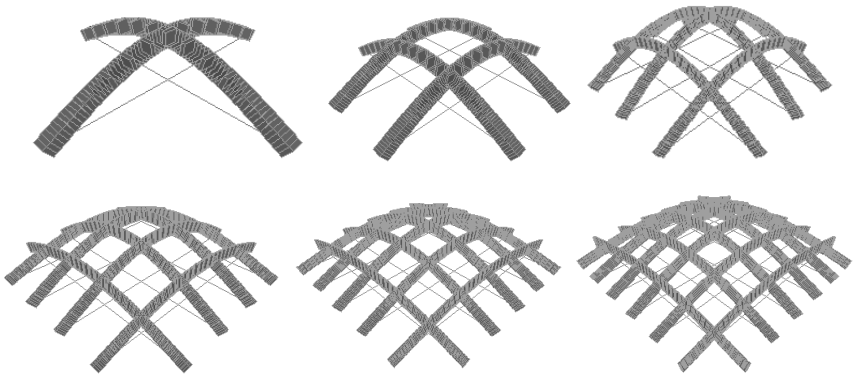

Fig. 6 Buckling mode shapes of grid systems (L_1/L_2=1.0), Load type 1

same mesh is also used for ANSYS solutions.The beams are assumed to be simply supported at the ends.

Biaxial uniform and triangular and uniaxial uniform inplane loads are considered. The loadings are depicted in Fig. 5.

Nondimensional out of plane buckling load parameters, $\lambda=12P_{cr}L_1L_2/(\pi^2E_tbh^3)$, are calculated

and given in tabular form.

In order to validate the element behavior for fully steel material, Load Type 1 and L_1/L_2=1.0 aspect ratio, results are compared with ANSYS commercial finite element program. It can be seen from Table 3 that although the presented element shows a stiffer behavior, the results are found to be in good agreement.

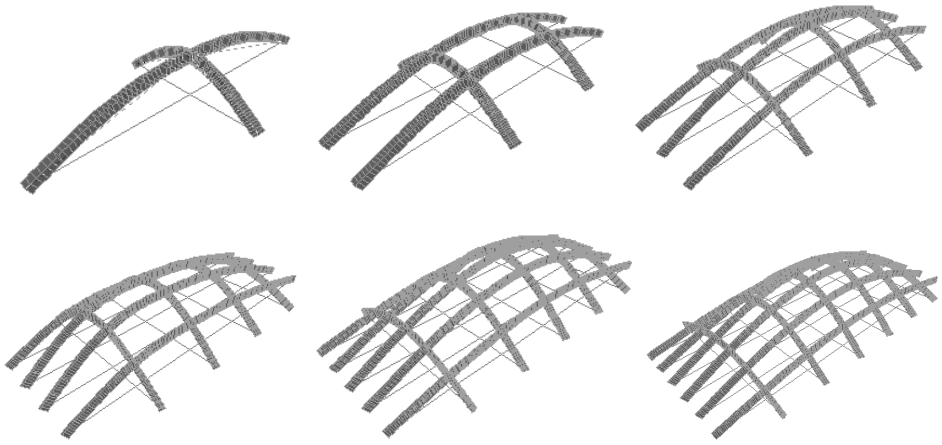

Fig. 7 Buckling mode shapes of grid systems (L_1/L_2=2.0), Load type 1

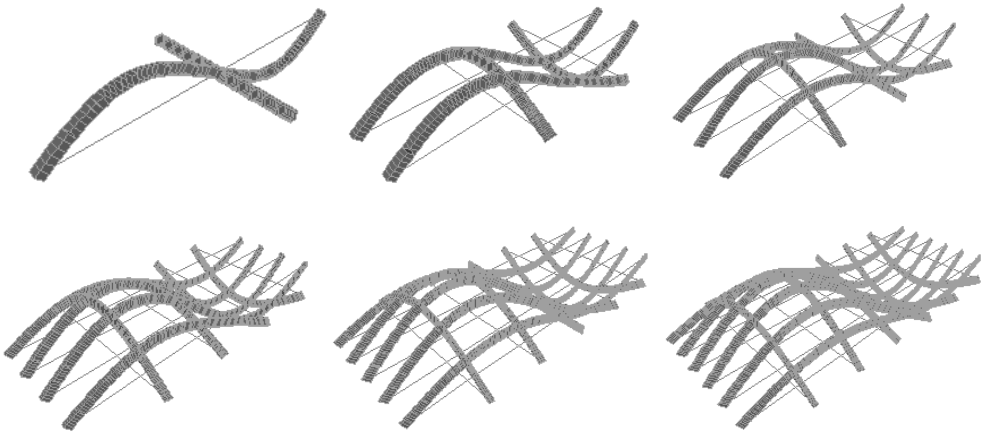

Fig. 8 Buckling mode shapes of grid systems (L_1/L_2=2.0) , Load type 3

Table 4 Nondimensional buckling load parameter λ, (L_1/L_2=1.0), Load type 2

	k=1/3	k=1	k=3	exp	Steel	Al_2O_3
M3	6.701	7.731	8.842	7.521	5.311	9.864
M4	5.425	6.234	7.098	6.072	4.310	8.005
M5	5.104	5.837	6.606	5.692	4.067	7.552
M6	4.995	5.688	6.405	5.553	3.989	7.408

Table 5 Nondimensional buckling load parameter λ, (L_1/L_2=2.0), Load type 1

	k=1/3	k=1	k=3	exp	Steel	Al_2O_3
M1	8.682	9.740	10.739	9.547	7.026	13.048
M2	9.331	10.632	11.972	10.374	7.451	13.837
M3	9.278	10.600	11.986	10.337	7.398	13.739
M4	9.167	10.441	11.767	10.192	7.323	13.598
M5	9.082	10.311	11.570	10.072	7.268	13.498
M6	9.020	10.212	11.420	9.983	7.230	13.428

Table 6 Nondimensional buckling load parameter λ, (L_1/L_2=2.0), Load type 2

	k=1/3	k=1	k=3	exp	Steel	Al_2O_3
M3	8.201	9.382	10.626	9.146	6.534	12.134
M4	7.953	9.066	10.225	8.847	6.349	11.792
M5	7.503	8.523	9.570	8.325	6.002	11.147
M6	7.372	8.350	9.341	8.161	5.908	10.971

Table 7 Nondimensional buckling load parameter λ, (L_1/L_2=1.0), Load type 3

	k=1/3	k=1	k=3	exp	Steel	Al_2O_3
M1	11.518	12.890	14.214	12.634	9.298	17.213
M2	12.717	14.673	16.676	14.288	10.147	18.845
M3	12.689	14.634	16.734	7.520	14.238	18.683
M4	12.460	14.311	16.287	13.941	9.902	18.391
M5	12.290	14.049	15.894	13.702	9.794	18.190
M6	12.144	13.826	15.564	13.498	7.495	18.016

Table 8 Nondimensional buckling load parameter λ, (L_1/L_2=2.0), Load type 3

	k=1/3	k=1	k=3	exp	Steel	Al_2O_3
M1	14.489	16.686	18.968	16.233	11.516	21.386
M2	18.653	21.366	24.196	20.821	14.844	27.566
M3	18.856	21.686	24.705	21.115	14.972	27.806
M4	18.613	21.344	24.242	20.799	14.804	27.495
M5	18.395	21.011	23.741	20.495	14.667	27.240
M6	18.194	20.704	23.291	20.215	14.537	26.999

The following observations can be made from the solutions. Indiviual or combined variation of aspect ratios, material distribution and loading type is found to have great influence on the stability of FGM grid systems.

The working range of k are taken as 1/3-3, any value outside this range are producing an FGM having too much of one phase. This can be also observed from the solutions that the buckling load parameter λ increase with the power-law exponent k. The results are getting closer to the full Al_2O_3 solutions.

It can be observed that among different types of material gradations functions, nondimensional parameter predicted by k=3 are the highest and k=1/3 lowest ones, respectively. For all cases, power law k=1 and exponential function results are close to each other.

Generally the buckling load parameters obtained from uniform load solutions are greater than the triangular load solutions. It can be seen from the Fig. 6, Fig. 7 and Fig. 8 that the mode shapes are different in uniaxial and biaxial loading.

The buckling load parameter λ values obtained from biaxial loadings are lower than the uniaxial loadings. This is because the existence of orthogonal compression forces are increasing the tendency of buckling.

5. Conclusions

An investigation of elastic buckling of FGM simply supported grid systems is presented. The analysis is carried out by using a hybrid stress beam finite element. It is assumed that the material properties of the beams vary continously in the thickness direction according to the exponential law and the power-law form. The effects of aspect ratio, type of gradations functions, type of inplane loading are discussed. It is observed that the above mentioned effects play very important role on the buckling behavior of the FGM grid systems. The tables given in this study combines the configurations of grid systems which are mostly used in practice, and will help a practicing engineer to choose an optimum solution considering both economy and other practical limitations.

References

ANSYS (1997), Swanson Analysis Systems, Swanson J. ANSYS 5.4, U.S.A.

Akgöz, B. and Civalek, Ö. (2014), "Shear deformation beam models for functionally graded microbeams with new shear correction factors", *Compos. Struct.*, **112**, 214-225.

Aydogdu, M. and Taskin, V. (2007), "Free vibration analysis of functionally graded beams with simply supported edges", *Mater. Des.*, **28**(5),1651-6.

Atmane, H.A., Tounsi, A., Ziane, N. and Mechab, I. (2011), "Mathematical solution for free vibration of sigmoid functionally graded beams with varying cross-section", *Steel Compos. Struct.*, **11**(6), 489-504.

Bouremana, M., Houari, M.S.A., Tounsi, A., Kaci, A. and Bedia, E.A. (2013), "A new first shear deformation beam theory based on neutral surface position for functionally graded beams", *Steel Compos. Struct.*, **15**(5), 467-479.

Cetin, D. and Simsek, M. (2011), "Free vibration of an axially functionally graded pile with pinned ends embedded in Winkler-Pasternak elastic medium", *Struct. Eng. Mech.*, **40**(4), 583-594.

Chakraborty, A., Gopalakrishnan, S. and Reddy, J.N. (2003), "A new beam finite element for the analysis of functionally graded materials", *Int. J. Mech. Sci.*, **45**, 519-539.

Chakraborty, A. and Gopalakrishnan, S. (2003), "A spectrally formulated finite element for wave propagation analysis in functionally graded beams", *Int. J. Solid. Struct.*, **40**(10), 2421-2448.

Ching, H.K. and Yen, S.C. (2005), "Meshless local Petrov-Galerkin analysis for 2D functionally graded elastic solids under mechanical and thermal loads", *J. Compos. Part B. Eng.*, **36**, 223-240.

Darilmaz, K. (2012), "Analysis of sandwich plates: a three-dimensional assumed stress hybrid finite element", *J. Sandw. Struct. Mater.*, 14(4), 487-501.

Darilmaz, K. (2011), "Influence of aspect ratio and fibre orientation on the stability of simply supported orthotropic skew plates", *Steel Compos. Struct.*, **11**(5), 359-374.

Darilmaz, K. (2015), "Vibration analysis of functionally graded material (FGM) grid systems", *Steel Compos. Struct.*, **18**(2), 395-408.

Giunta, G., Koutsawa, Y., Belouettar, S. and Calvi, A. (2014), "A dynamic analysis of three-dimensional functionally graded beams by hierarchical models", *Smart Struct. Syst.*, **13**(4), 637-657.

Kapuria, S., Bhattacharyya, M. and Kumar, A.N. (2008), "Bending and free vibration response of layered functionally graded beams: a theoretical model and its experimental validation", *Compos. Struct.*, **82**(3), 390-402.
Kim, J. and Paulino, G.H. (2002), "Finite element evaluation of mixed mode stress intensity factors in functionally graded materials", *Int. J. Numer. Meth. Eng.*, **53**(8), 1903-1935.
Kocaturk, T. and Akbas, S.D. (2013), "Thermal post-buckling analysis of functionally graded beams with temperature-dependent physical properties", *Steel Compos. Struct.*, **15**(5), 481-505.
Li, X.F. (2008), "A unified approach for analyzing static and dynamic behaviors of functionally graded Timoshenko and Euler-Bernoulli beams", *J. Sound Vib.*, **318**(4-5), 1210-1229.
Li, S.R. and Batra, R.C. (2013), "Relations between buckling loads of functionally graded Timoshenko and homogeneous Euler-Bernoulli beams", *Compos. Struct.*, **95**, 5-9.
Lu, C.F. and Chen, W.Q. (2005), "Free vibration of orthotropic functionally graded beams with various end conditions", *Struct. Eng. Mech.*, **20**(4), 465-476.
Lü, C.F., Chen, W.Q., Xu, R.Q. and Lim, C.W. (2008), "Semi-analytical elasticity solutions for bi-directional functionally graded beams", *Int. J. Solid. Struct.*, **45**, 258-275.
Pian, T.H.H. and Chen, D.P. (1983), "On the suppression of zero energy deformation modes", *Int. J. Numer. Meth. Eng.*, **19**, 1741-1752.
Qian, L.F. and Ching, H.K. (2004), "Static and dynamic analysis of 2D functionally graded elasticity by using meshless local Petrov-Galerkin method", *J. Chinese Inst. Eng.*, **27**, 491-503.
Sanjay Anandrao, K., Gupta, R.K., Ramchandran, P. and Venkateswara Rao, G. (2012), "Non-linear free vibrations and post- buckling analysis of shear flexible functionally graded beams", *Struct. Eng. Mech.*, **44**(3), 339-361.
Sankar, B.V. (2001), "An elasticity solution for functionally graded beams", *Compos. Sci. Technol.*, **61**(5), 689-696.
Simsek, M. and Reddy, J.N. (2013), "A unified higher order beam theory for buckling of a functionally graded microbeam embedded in elastic medium using modified couple stress theory", *Compos. Struct.*, **101**, 47-58.
Şimşek, M. (2009), "Static analysis of a functionally graded beam under a uniformly distributed load by Ritz method", *Int. J. Eng. Appl. Sci.*, **1**(3), 1-11.
Şimsek, M. and Kocatürk, T. (2009), "Free and forced vibration of a functionally graded beam subjected to a concentrated moving harmonic load", *Compos. Struct.*, **90**, 465-473.
Şimsek, M. (2010), "Vibration analysis of a functionally graded beam under a moving mass by using different beam theories", *Compos. Struct.*, **92**, 904-917.
Tajalli, S.A., Rahaeifard, M., Kahrobaiyan, M.H., Movahhedy, M.R., Akbari, J. and Ahmadian, M.T. (2013), "Mechanical behavior analysis of size-dependent micro-scaled functionally graded Timoshenko beams by strain gradient elasticity theory", *Compos. Struct.*, **102**, 72-80.
Wakashima, K., Hirano, T. and Niino, M. (1990), "Space applications of advanced structural materials", ESA, SP-303, 97.
Xiang, H.J. and Yang, J. (2007), "Free and forced vibration of a laminated FGM Timoshenko beam of variable thickness under heat conduction", *J. Compos. Part B*, **39**(2), 292-303.
Ying, J., Lü, C.F. and Chen, W.Q. (2008), "Two-dimensional elasticity solutions for functionally graded beams resting on elastic foundations", *Compos. Struct.*, **84**(3), 209-219.
Yang, J. and Chen, Y. (2008), "Free vibration and buckling analyses of functionally graded beams with edge cracks", *Compos. Struct.*, **83**(1), 48-60.
Yang, J., Chen, Y., Xiang, Y. and Jia, X.L. (2008), "Free and forced vibration of cracked inhomogeneous beams under an axial force and a moving load", *J. Sound Vib.*, **312**(1-2), 166-181.
Zhong, Z. and Yu, T. (2007), "Analytical solution of a cantilever functionally graded beam", *Compos. Sci. Technol.*, **67**(3-4), 481-488.

Notations

b : width
h : thickness
k : power-law exponent
E : modulus of elasticity
L_1, L_2 : length of the grid system
P_{cr} : critical load
V : volume
λ : nondimensional critical load parameter
$[D]$: differential operator matrix
$[G]$: nodal forces corresponding to assumed stress field
$[K]$: stiffness matrix
$[N]$: shape functions
$[P]$: interpolation matrix for stress
$[S]$: material compliance matrix
$\{q\}$: displacement components
$\{u\}$: displacements
$\{\beta\}$: stress parameters
$\{\sigma\}$: stress
$\{\varepsilon\}$: strain